Synthesis and Characterization of Polyurethane Hybrids: Influence of the Polydimethylsiloxane Linear Chain and Silsesquioxane Cubic Structure on the Thermal and Mechanical Properties of Polyurethane Hybrids

K. Madhavan, B. S. R. Reddy

Industrial Chemistry Laboratory, Central Leather Research Institute, Chennai 600 020, India

Received 28 December 2007; accepted 22 March 2009
DOI 10.1002/app.30494
Published online 27 May 2009 in Wiley InterScience (www.interscience.wiley.com).

ABSTRACT: The structural effects of polydimethylsiloxane (PDMS) or polyhedral oligosilsesquioxanes (POSSs) on the thermomechanical properties of polyurethane (PU) networks were studied. An ester–amine-functionalized silsesquioxane and a PDMS macromer were synthesized, and the macromer (10 wt %) was crosslinked with the PU prepolymer to obtain PU networks. The synthesized macromers and hybrids were characterized with Fourier transform infrared, ^{1}H-NMR, ^{13}C-NMR, and ^{29}Si-NMR spectroscopy techniques. The influence of POSS cubes on the thermal and mechanical properties of the polymer network films was studied comparatively with the similarly functionalized PDMS linear chain via thermogravimetric analysis (TGA), differential scanning calorimetry (DSC), and dynamic mechanical analysis (DMA) measurements. The degradation pattern of the POSS-incorporated PU nanocomposites was almost the same as that of the PU network synthesized from the linear PDMS macromer. The differences in the char yields and activation energies of the hybrids reflected the enhancement of the thermal properties of the nanohybrids. The TGA and DSC curves of the macromers suggested that the thermal properties of the macromers not only depended on either the PDMS or POSS inorganic core but also depended on the organic peripheral attached to the inorganic core. The glass-transition temperatures of the nanohybrids were higher than those of the linear-PDMS-incorporated hybrids. The storage modulus values increased 3-fold upon the incorporation of POSS rigid groups into the PU hybrids in comparison with the flexible PDMS-chain-incorporated PU hybrids. The DMA measurements showed a long-range rubbery plateau region for all the PU hybrids, with high storage modulus and tan δ values showing the structural homogeneity of the crosslinked networks. J Appl Polym Sci 113: 4052–4065, 2009

Key words: nanocomposites; polysiloxanes; polyurethanes

INTRODUCTION

Polyurethane (PU) is a versatile polymer that can be prepared by a simple polyaddition reaction of polyol, isocyanate, and a chain extender.[1–3] Unfortunately, conventional PU is known to exhibit little resistance to heat, and this limits its applications. Previously, attempts to improve the thermal stability of PU have involved either the modification of the chemical structure by blending or copolymerization or grafting to more thermally stable polymers such as polydimethylsiloxane (PDMS)[4] and polyimides.[5] Chemical modification of PU by copolymerization with other monomers has some disadvantages: the copolymer tends to lower the individual properties of PU. For example, the mechanical properties of PU are reduced by copolymerization with a siloxane soft segment, and the insoluble nature of polyamides and polyimides limits the applications of PU processing.

In recent years, nanocomposites with improved thermal and mechanical properties have been studied extensively. Nanocomposites are composite materials consisting of building blocks on the scale of nanometers or tens of nanometers, and the nanoparticles can be either chemically bonded or blended.[6] Various PU nanocomposites have been prepared with different types of nanoparticles such as ZnO, clay, and especially polyhedral oligosilsesquioxane (POSS).[7–10] POSS is a hybrid nanostructured macromer widely used in the preparation of polymeric nanocomposites.[11–18] POSS molecules are an interesting class of clusters derived from the hydrolytic condensation of trifunctional organosilicon monomers.[19,20] The term *silsesquioxane* is used to denote materials containing on average 1 silicon atom bound to 1.5 oxygen atoms and 1 R group

Correspondence to: B. S. R. Reddy (induchem2000@yahoo.com).

Contract grant sponsors: Council of Scientific and Industrial Research (through a senior research fellowship to K.M. and DST); contract grant number: SR/SI/PC-33/2006.

(where R may be an organofunctional groups) and having the general formula $[RSiO_{3/2}]_n$ (n is an even integer ≥ 4).

POSS can be incorporated into a polymer matrix via physical blending or covalent bonding with polymers. Covalently bonded POSS nanocomposites exhibit improved thermal and mechanical properties, increased glass-transition temperature (T_g) values, and decreased dielectric constants for hybrid inorganic/organic nanocomposites.[21–23] POSS molecules are also used as nanocatalyst supports and have excellent biomedical applications.[24,25] POSS functionalized with eight identical groups can be reacted to form a material with a high crosslink density. The functional groups that have been used in the preparation of crosslinked hybrid materials include epoxy,[26] amine,[27] methacryloyl,[28] vinyl,[29] and hydroxyl groups.[30]

Very few reports have been available in the literature about PU hybrids using POSS systems because the functionalization of a POSS macromer to form PU nanocomposites is difficult. However, researchers have found various synthetic routes to functionalize POSS molecules suitable for obtaining PU–POSS hybrids.[9,10,31–34] In this work, we employed a different route for the synthesis of amine-functionalized POSS and a POSS molecule suitable for the synthesis of PU–POSS nanocomposites. The purpose of incorporating POSS was to determine the structural effect of the POSS cage molecule and linear PDMS chain on the thermal and mechanical properties of PU. The influence of the POSS cage structure on the thermal and mechanical properties of hybrids was compared with composites synthesized from a similarly functionalized linear PDMS macromer. To prepare organic/inorganic hybrid polymers, we incorporated 10 wt % POSS or linear PDMS macromer as a crosslinker into hybrids. The structural effect of POSS or PDMS on the thermomechanical properties of PU networks was studied on the basis of dynamic mechanical analysis (DMA), thermogravimetric analysis (TGA), and differential scanning calorimetry (DSC) analysis.

EXPERIMENTAL

Materials and measurements

Octakis(dimethylsilyl)silsesquioxane ($Q_8M_8^H$) was synthesized by the adoption of a modified literature procedure.[35,36] Polyhydromethylsiloxane (PHMS) with a number-average molecular weight of 1900 and 2-allyloxyethanol were obtained from Lancaster and used as received. Tetraethoxysilane, tetramethylammonium hydroxide, chlorodimethylsilane, allyl alcohol, 4-nitrobenzoyl chloride, poly(ethylene glycol) (PEG; number-average molecular weight = 1000), aminopropyl-terminated PDMS (number-average molecular weight = 2500), and platinum divinyltetramethyl disiloxane complex [Pt(dvs); used as a catalyst] were obtained from Aldrich (St. Louis, MO). Methylene diphenyl diisocyanate (MDI; Merck, Mumbai, India) and dibutyl tin dilaurate (DBTDL; Aldrich) were used as received. Solvents such as toluene and dimethylformamide were dried with calcium hydride.

Characterization

IR spectra were recorded with a PerkinElmer Fourier (USA) transform infrared (FTIR) spectrometer with the KBr pellet technique.

^{1}H-, ^{13}C-, and ^{29}Si-NMR spectra were recorded with $CDCl_3$ or hexadeuterated dimethyl sulfoxide (DMSO-d_6) as the solvent and tetramethylsilane as the internal standard on a JEOL 500-MHz instrument (Peabody, MA).

Electron spray ionization was performed with a Thermo Fennigan mass spectrometer (Canton, MA). Elemental analysis data were recorded with a Euro-Vector elemental analyzer (Milan, Italy). Thermal analyses were performed with a PerkinElmer DSC TGA-7 under a nitrogen flow. The average activation energy (E_a) values of the PU hybrids were calculated at various heating rates (5, 10, 15, and 20°C/min).

Dynamical mechanical tests were carried out under an N_2 atmosphere with a Netzsch DMA 242 mechanical analyzer (Selb, Germany) on $25 \times 5 \times 0.5$ mm^3 samples at a frequency of 0.1 Hz from −100 to 250°C with a heating rate of 5°C.

The surface morphology of PU nanohybrids was studied with a Nanoscope III atomic force microscopy (AFM, Santa Barbara, CA) instrument, and imaging was performed in the contact mode at room temperature in air. In these studies, we used a commercial tip of Si_3N_4 provided by Digital Instruments. The cantilever length was 200 μm, and the spring constant was 0.12 N/m.

Synthesis of allyl 4-nitrobenzoate (2a)

Triethylamine (20 mL, 0.15 mol) was added to a solution of **1a** (5.8 g, 0.1 mol; Scheme 1) in 10 mL of dried toluene and then heated to 50°C. A solution of 4-nitrobenzoyl chloride (18.5 g, 0.1 mol) in toluene was added dropwise over 30 min, and the mixture was refluxed for 5 h. The reaction mixture was allowed to cool to room temperature and filtered to remove the precipitate. Finally, the filtrate was washed with a 5% aqueous $NaHCO_3$ solution (40 mL). Then, the toluene phase was separated, and the product was concentrated. **2a** (Scheme 1) was obtained (90% yield) as a light, pale green liquid.

IR (cm^{-1}): 2946 (C—H stretch), 1726 (C=O stretch), 1273 (O—C=O), 1602 (C=C stretch), 1529

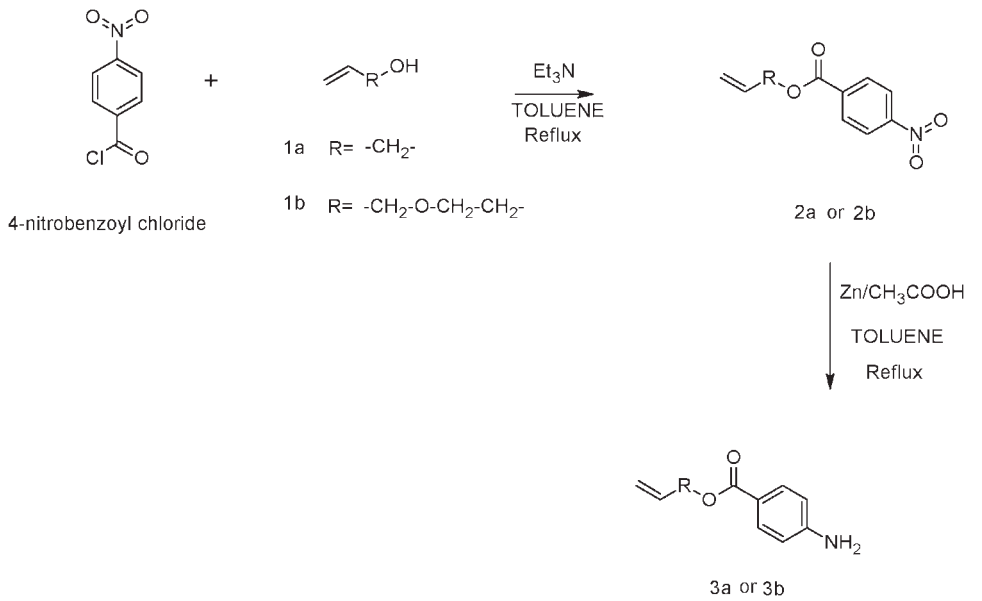

Scheme 1 Synthesis of **3a** and **3b**.

and 1348 (N—O stretch), 868 and 504 (aromatic ring stretch). ^{1}H-NMR (500 MHz, $CDCl_3$, ppm): 5.37 and 5.41 (d CH_2=CH), 6.01 (m CH_2=CH), 4.82 (d CH_2—O), 8.22 and 8.18 (d Ar C—H). ^{13}C-NMR (500 MHz, $CDCl_3$, ppm): 119.14 (CH_2=CH), 135.56 (CH_2=CH), 66.50 (CH_2—O), 131.62, 130.81, 123.60, and 150.60 (Ar—C), 164.38 (—C=O). m/z: 207 (M^+). ANAL. Calcd for $C_{10}H_9NO_4$: C, 57.97%; H, 4.38%; N, 6.76%. Found: C, 56.12%; H, 3.91%; N, 6.19%.

Synthesis of allyl(oxy)ethyl 4-nitrobenzoate (2b)

The same procedure used in the synthesis of **2a** was followed to obtain **2b**. A pale green, waxy liquid was obtained (85% yield).

IR (cm^{-1}): 2921 (C—H stretch), 1720 (C=O stretch), 1276 (O—C=O), 1599 (C=C stretch), 1528 and 1340 (N—O stretch), 1104 (C—O—C stretch), 868 and 719 (aromatic ring stretch). ^{1}H-NMR (500 MHz, $CDCl_3$, ppm): 5.28 and 5.16 (d CH_2=CH), 5.88 (m CH_2=CH), 4.56 (t CH_2—CH_2—O—C=O), 4.04 (t CH_2—CH_2—O—C=O), 3.77 (d CH—CH_2—O), 8.23 and 8.19 (d Ar C—H). ^{13}C-NMR (500 MHz, $CDCl_3$, ppm): 117.57 (CH_2=CH), 135.54 (CH_2=CH), 72.21 (CH_2—CH_2—O—C=O), 67.77 (CH_2—CH_2—O—C=O), 65.08 (CH—CH_2—O), 134.36, 131.08, 123.57, and 150.61 (Ar—C), 164.74 (—C=O). m/z: 251 (M^+). ANAL. Calcd for $C_{12}H_{13}NO_5$: C, 57.37%; H, 5.22%; N, 5.57%. Found: C, 55.20%; H, 4.91%; N, 5.35%.

Synthesis of allyl 4-aminobenzoate (3a)

A 500-mL, three-necked, round-bottom flask fitted with a dropping funnel, a condenser, and a stirrer was charged with 19.5 g (0.3 mol) of activated Zn (activated by stirring in 30 mL of 5% aqueous HCl for 2 min and washed then with 100 mL of water and finally 30 mL of MeOH) and ammonium formate (18.0 g, 0.3 mol) in 50 mL of toluene. A solution of **2a** (20.7 g 0.1 mol) in acetic acid (17.7.mL, 0.3 mol) was added dropwise over 30 min, and refluxing was continued for 12 h. The mixture was then neutralized with $NaHCO_3$ and filtered while hot. When the filtrate was washed with water, the toluene phase was separated, and the product was concentrated to give an orange-brown solid (70% yield).

IR (cm^{-1}): 2946 (C—H stretch), 1691 (C=O stretch), 1637 (C=C stretch), 3420, 3334, and 3216 (N—H stretch), 1276 (O—C=O), 3095, 842, and 561 (aromatic ring stretch). ^{1}H-NMR (500 MHz, $CDCl_3$, ppm): 5.39 and 5.23 (d CH_2=CH), 6.04 (m CH_2=CH), 4.75 (d CH_2—O), 4.09 (s, NH_2), 7.87 and 6.62 (d Ar C—H). ^{13}C-NMR (500 MHz, $CDCl_3$, ppm): 119.66 (CH_2=CH), 132.80 (CH_2=CH), 65.08 (CH_2—O), 113.87, 131.79, 117.81, and 151.05 (Ar—C), 166.43 (—C=O). m/z: 177 (M^+). ANAL. Calcd for $C_{10}H_{11}NO_2$: C, 67.78%; H, 6.26%; N, 7.90%. Found: C, 66.55%; H, 5.95%; N, 7.60%.

Synthesis of allyl(oxy)ethyl 4-aminobenzoate (3b)

The synthetic procedure adopted for **3a** was used for the synthesis of **3b**. An orange-brown liquid was obtained (70% yield).

IR (cm^{-1}): 2865 (C—H stretch), 1696 (C=O stretch), 1275 (O—C=O), 1603 (C=C stretch), 3367 (N—H stretch), 1023 (C—O—C stretch), 845 and 771 (aromatic ring stretch). ^{1}H-NMR (500 MHz, $CDCl_3$, ppm): 5.29 and 5.19 (d CH_2=CH), 5.90 (m CH_2=CH), 4.39 (t CH_2—CH_2—O), 4.03 (t CH_2—CH_2—O), 3.73 (d CH—CH_2—O), 4.10 (s, NH_2),

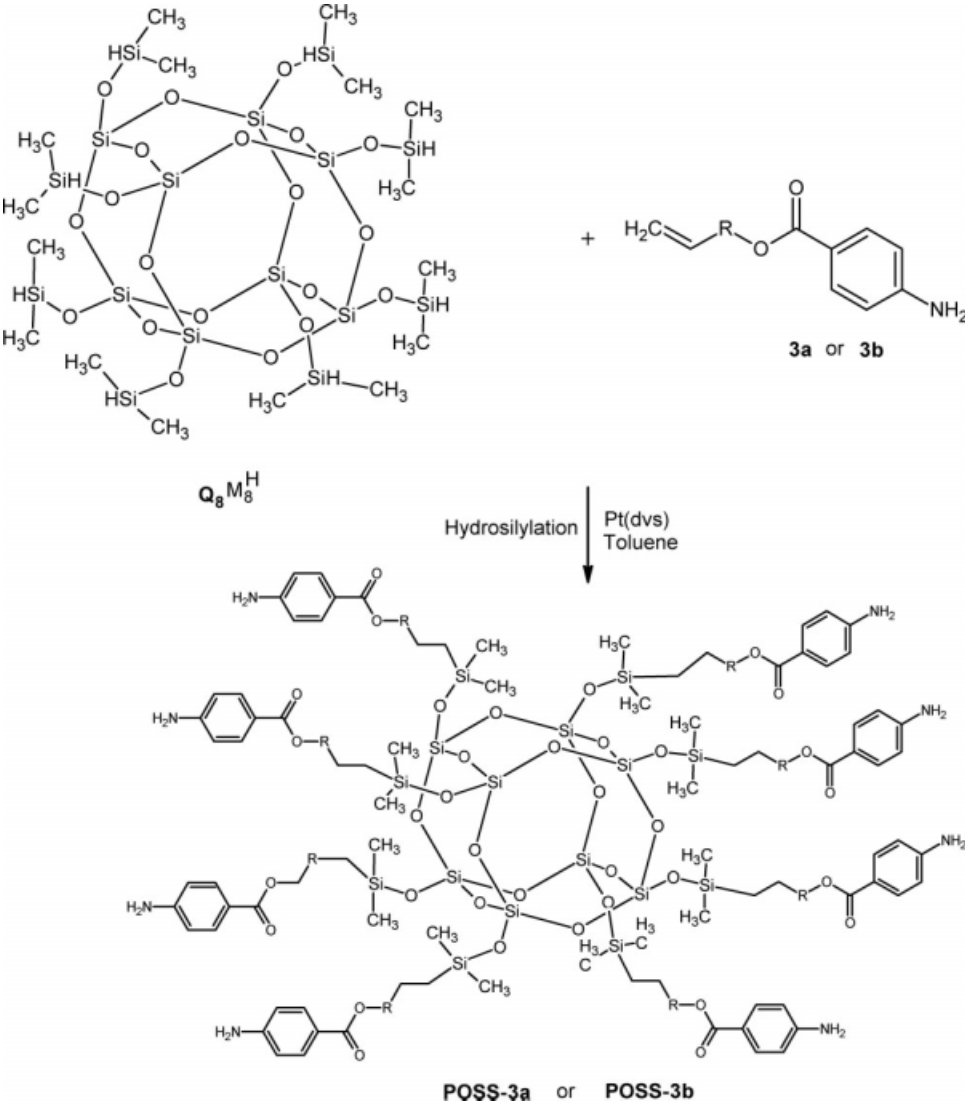

Scheme 2 Synthesis of POSS–**3a** and POSS–**3b**.

7.82 and 6.65 (d Ar C—H). ^{13}C-NMR (500 MHz, $CDCl_3$, ppm): 119.39 (CH_2=CH), 134.59 (CH_2=CH), 72.21 (CH_2—CH_2—O), 68.27 (CH_2—CH_2—O), 63.71 (CH—CH_2—O), 113.82, 131.83, 117.46, and 151.22 (Ar—C), 166.81 (—C=O). m/z: 221 (M^+). ANAL. Calcd for $C_{12}H_{15}NO_3$: C, 65.14%; H, 6.83%; N, 6.33%. Found: C, 64.34%; H, 6.28%; N, 6.06%.

Synthesis of POSS–3a

Into a two-necked, 100-mL, round-bottom flask equipped with a reflux condenser and N_2 inlet were placed $Q_8M_8^H$ (1 g, 0.98 mmol), **3a** (1.74 g, 9.82 mmol), and dried toluene (20 mL). Karstedt's catalyst [Pt(dvs); 20 μL] was then added, and the reaction was carried out for 12 h at room temperature under an atmosphere of N_2. A brown, waxy liquid settled on the sides of the flask after 12 h. Then, the toluene phase was removed, and the waxy liquid was washed thoroughly with toluene. The trapped solvent in the product was removed under reduced pressure. A brownish-yellow solid was obtained (75% yield).

IR (cm^{-1}): 2961 (C—H stretch), 1679 (C=O stretch), 3370 (N—H stretch), 1283 (O—C=O), 1103 (Si—O—Si stretch), 845 and 555 (aromatic ring stretch). ^{1}H-NMR (500 MHz, DMSO-d_6, ppm): 0.02 (s, —Si—CH_3), 1.61 (m, CH_2—CH_2—Si), 0.55 (t, —CH_2—Si), 4.01 (s NH_2), 5.83 (t, —O—CH_2), 6.51 and 7.58 (d Ar C—H). ^{13}C-NMR (500 MHz, DMSO-d_6, ppm): 0.23 (—Si—CH_3), 13.53 (—CH_2—Si), 22.55 (CH_2—CH_2—Si), 66.54 (—O—CH_2), 113.09, 131.75, 117.37, 153.88 (Ar—C), 168.05 (—C=O). ^{29}Si-NMR (500 MHz, DMSO-d_6, ppm): 13.60 (Si—CH_2), −108.05 (SiO_4). ANAL. Calcd for $C_{96}H_{144}N_8O_{36}Si_{16}$: C, 48.73%; H, 5.98%; N, 4.82%. Found: C, 48.10%; H, 5.45%; N, 4.24%.

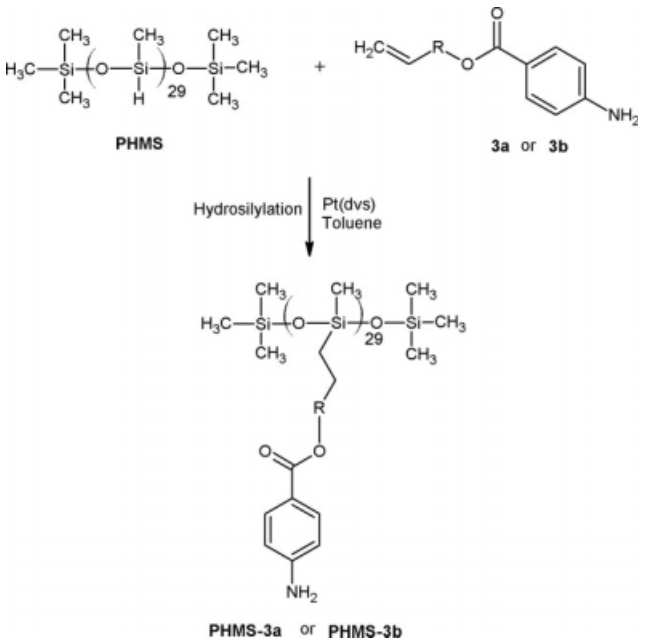

Scheme 3 Synthesis of PHMS–**3a** and PHMS–**3b**.

Synthesis of POSS–3b

The same reaction conditions adopted for POSS–**3a** were used for the synthesis of POSS–**3b**. A slight modification of the reaction procedure was carried out. The reaction mixture was heated to 60°C to obtain a clear liquid before the addition of the catalyst and then was cooled to room temperature. After 30 min, 20 μL of the catalyst was added, and the reaction was continued for 12 h. A dark brown, waxy liquid settled on the bottom of the flask, which was washed with toluene and vacuum-dried. A brownish-black, waxy liquid was obtained (70% yield).

IR (cm^{-1}): 2954 (C—H stretch), 1693 (C=O stretch), 3370 (N—H stretch), 1276 (O—C=O), 1105 (Si—O—Si stretch), 1024 (C—O—C stretch), 843 and 772 (aromatic ring stretch). ^{1}H-NMR (500 MHz, $CDCl_3$, ppm): 0.09 (s, —Si—CH_3), 0.58 (t, —CH_2—Si), 1.57 (m, CH_2—CH_2—Si), 3.42 (t, CH_2—CH_2—CH_2—O), 4.37 (t, CH_2—CH_2—O—C=O), 3.69 (t, CH_2—CH_2—O—C=O), 4.10 (s NH_2), 7.83 and 6.59 (d Ar C—H). ^{13}C-NMR (500 MHz, $CDCl_3$, ppm): −0.31 (—Si—CH_3), 13.69 (—CH_2—Si), 23.20 (CH_2—CH_2—Si), 63.78 (CH_2—CH_2—CH_2—O), 68.86 (CH_2—CH_2—O—C=O), 74.02 (CH_2—CH_2—O—C=O), 113.80, 131.81, 119.44, and 151.19 (Ar—C), 166.78 (—C=O). ^{29}Si-NMR (500 MHz, $CDCl_3$, ppm): 13.60 (Si—CH_2), −108.52 (SiO_4). ANAL. Calcd for $C_{112}H_{176}N_8O_{44}Si_{16}$: C, 48.25%; H, 6.36%; N, 4.02%. Found: C, 47.43%; H, 5.92%; N, 3.54%.

Synthesis of PHMS–3a

PHMS (1.9 g, 1.0 mmol), **3a** (5.3 g, 29.99 mmol), and dried toluene (20 mL) were placed in a 100-mL, two-necked, round-bottom flask equipped with a reflux condenser under an atmosphere of N_2. To this, 20 μL of Pt(dvs) was added, and the reaction was carried out for 3 h. A brown precipitate was formed, and it was filtered and washed with toluene. Then, the product was vacuum-dried at 60°C for 10 h. A brown, spongy solid was obtained (72% yield).

IR (cm^{-1}): 2952 (C—H stretch), 1679 (C=O stretch), 3367 (N—H stretch), 1283 (O—C=O), 1102 (Si—O—Si stretch), 897 and 770 (aromatic ring stretch). ^{1}H-NMR (500 MHz, DMSO-d_6, ppm): 0.03 (s, —Si—CH_3), 1.63 (m, CH_2—CH_2—Si), 0.51 (t, —CH_2—Si), 4.01 (s NH_2), 5.85 (t, —O—CH_2), 6.51 and 7.58 (d Ar C—H). ^{13}C-NMR (500 MHz, DMSO-d_6, ppm): −0.13 (—Si—CH_3), 13.53 (—CH_2—Si), 22.55 (CH_2—CH_2—Si), 66.54 (—O—CH_2), 112.09, 132.75, 117.37, and 152.81 (Ar—C), 168.05 (—C=O). ANAL. Calcd for $C_{112}H_{176}N_8O_{44}Si_{16}$: C, 55.40%; H, 6.43%; N, 5.76%. Found: C, 54.24%; H, 5.85%; N, 5.21%.

Synthesis of PHMS–3b

The procedure described for PHMS–**3a** was used for the synthesis of PHMS–**3b**. The reaction mixture was heated to 60°C to obtain a clear brown solution before the addition of the catalyst and then was cooled to room temperature. After 30 min, 20 μL of the Pt(dvs) catalyst was added to the cooled reaction mixture. Then, the reaction was carried out for 4 h. A yellowish-brown, waxy liquid settled on the bottom of the flask, and it was separated and washed with toluene. The product was dried at 60°C for 12 h to remove traces of the solvent (73% yield).

IR (cm^{-1}): 2942 (C—H stretch), 1696 (C=O stretch), 3368 (N—H stretch), 1277 (O—C=O), 1102 (Si—O—Si stretch), 1053 (C—O—C stretch), 850 and 770 (aromatic ring stretch). ^{1}H-NMR (500 MHz, DMSO-d_6, ppm): 0.02 (s, —Si—CH_3), 0.39 (t, —CH_2—Si), 1.45 (m, CH_2—CH_2—Si), 3.28 (t, CH_2—CH_2—CH_2—O), 3.51 (t, CH_2—CH_2—O—C=O), 5.85 (t, CH_2—CH_2—O—C=O), 4.15 (s NH_2), 7.57 and 6.53 (d Ar C—H). ^{13}C-NMR (500 MHz, DMSO-d_6, ppm): −0.15 (—Si—CH_3), 13.43 (—CH_2—Si), 23.18 (CH_2—CH_2—Si), 63.41 (CH_2—CH_2—CH_2—O), 68.59 (CH_2—CH_2—O—C=O), 73.28 (CH_2—CH_2—O—C=O), 113.08, 131.61, 116.31, and 153.93 (Ar—C), 166.32 (—C=O). ANAL. Calcd for $C_{112}H_{176}N_8O_{44}Si_{16}$: C, 55.27%; H, 6.84%; N, 4.88%. Found: C, 54.95%; H, 6.45%; N, 4.51%.

Synthesis of PU hybrids

PEG (1.0 g, 1.0 mmol), 1.0 g (0.40 mmol) of aminopropyl-terminated PDMS, 0.7 g (2.8 mmol) of MDI, and 30 mL of dried toluene were charged into a 100-mL, three-necked, round-bottom flask equipped with a mechanical stirrer and a nitrogen inlet. The reaction was performed under a nitrogen atmosphere at 80°C for 5 h to produce the PU prepolymer.

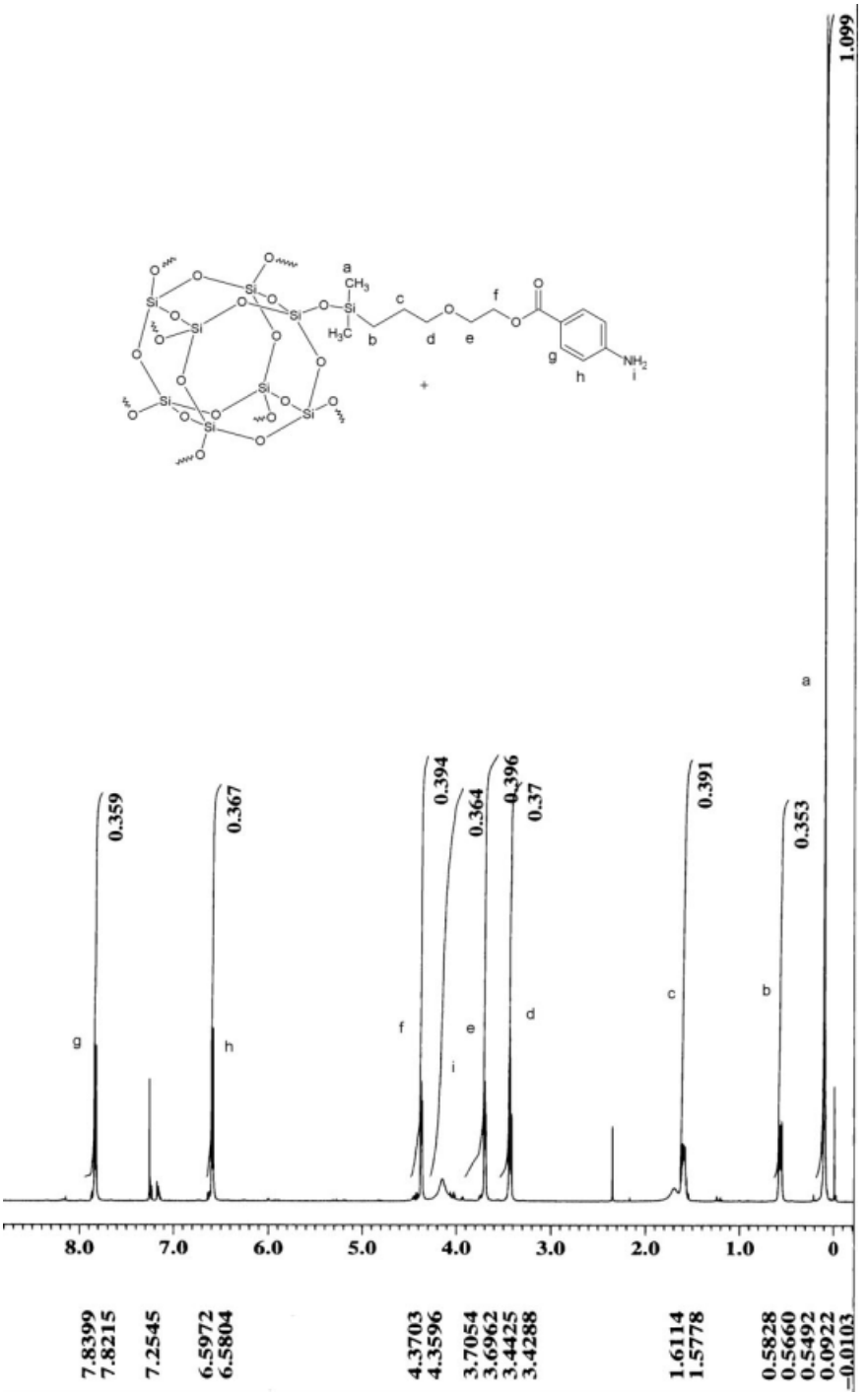

Figure 1 ^{1}H-NMR spectrum of POSS–**3b**.

POSS–**3a** (0.3 g, 0.12 mmol), dissolved in 10 mL of dried *N*,*N*′-dimethylformamide, was added to the PU prepolymer at 80°C with vigorous stirring. To this reaction mixture, 20 μL of the DBTDL catalyst was added. After 30 min, the reaction mixture became viscous; it was vigorously stirred and then cast into films in a Teflon-coated petri dish. Subsequently, the solution was cured at 100°C for 2 h and at 120°C for 3 h. Then, the films were peeled from the petri dish and dried for 24 h at 120°C. The same procedure was followed for the synthesis of PU–POSS–**3b**, PU–PHMS–**3a**, and PU–PHMS–**3b** with 10 wt % concentrations of the POSS–**3b**, PHMS–**3a**, and PHMS–**3b** macromers, respectively.

RESULTS AND DISCUSSION

Synthesis of the macromers

To synthesize POSS-incorporated hybrid materials, the functionalization of the POSS molecule is

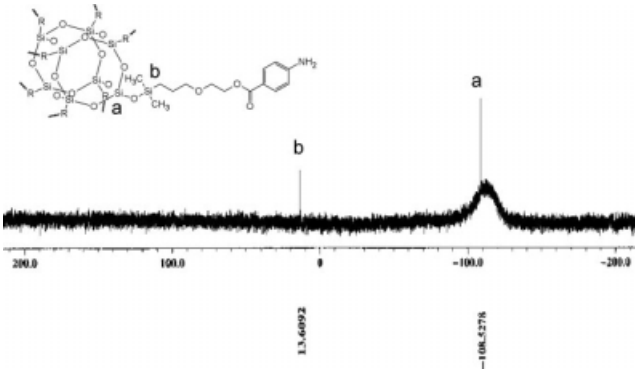

Figure 2 ^{29}Si-NMR spectrum of POSS–**3b**.

essential. To graft a functional group into the POSS molecule, the hydrosilylation reaction is the best tool. Hence, we grafted **3a** or **3b** to a POSS ($Q_8M_8^H$) molecule (Scheme 2) through a hydrosilylation reaction with the Pt(dvs) catalyst in the presence of toluene as the medium. Similarly, PHMS was reacted with **3a** or **3b** (Scheme 3) through a hydrosilylation reaction. The synthesized macromer was well confirmed with FTIR and ^{1}H-NMR on the basis of the Si—H band at 2100 cm^{-1} and the chemical shift at 4.7 ppm, which fully disappeared and showed complete substitution in the POSS molecule and also in the PHMS molecule. The ^{1}H-NMR spectrum of POSS–**3b** is shown in Figure 1. The POSS-functionalized macromer was further characterized with the ^{29}Si-NMR spectroscopic technique. Figure 2 shows two chemical shift values corresponding to the two types of silicon atoms present in the macromer. The chemical shift at 13.6 ppm corresponds to the silicon atom present in the outer core bonded to the POSS cube, and the shift at −108.52 ppm is due to the silicon atom present in the core. The presence of these two chemical shifts confirms the complete substitution in the POSS molecule, which further supports the idea that the cube structure of POSS remains unaltered during the hydrosilylation reaction.

Solubility behavior of the macromers

The solubility behavior of the synthesized macromers was studied in various solvents and is shown in Table I. The macromers POSS–**3a**, PHMS–**3a**, and PHMS–**3b** were soluble only in solvents such as dimethyl sulfoxide, *N*,*N*′-dimethylformamide, and *N*-methylpyrrolidone. The macromer POSS–**3b** was highly soluble in most of the solvents except toluene and hexane. This may have been due to the substitution of a higher alkane chain and the presence of an ether linkage in the POSS molecule. In the case of POSS–**3a**, the substituted alkane chains were short and less soluble. However, the solubility of PHMS–**3a** and the solubility of PHMS–**3b** were almost the same in all the solvents. This shows that the solubility behavior not only is governed by the organic substituents but also depends on the Si—O—Si structural framework of the siloxane group. From Table I, it can be concluded that the POSS macromers were more soluble than the linear PHMS-substituted macromers. Even for the POSS-substituted macromers, the solubility depended on the chain length of the organic tethers and the nature (e.g., ether linkage) of the organic tethers.

Preparation of the nanocomposites

The nanocomposites were prepared via the crosslinking of the PU prepolymer with the amine-functionalized POSS macromer. The thermal and mechanical properties of the nanocomposites were compared with those of hybrids obtained from the linear amine-functionalized PDMS macromer. The prepolymer was synthesized through the reaction of the MDI hard segment with PEG and aminopropyl-terminated PDMS soft segments. To study the effect of the nanocrosslinker, all the hybrids were synthesized via the crosslinking of 50 wt % PEG prepolymer and 40 wt % PDMS prepolymer with the respective macromers (10 wt %). The crosslinked chemical structures of the POSS- and PHMS-incorporated hybrids are shown in Schemes 4 and 5. In this work, PDMS and PEG bisoft segments were used to obtain a hybrid film with good thermomechanical properties. Reports show that bisoft segmented hybrids have better mechanical properties than individual soft segments.[37] The chemical structures of the hybrids were elucidated with the FTIR technique.

Figure 3 shows the FTIR spectra of PU hybrids containing POSS and linear PDMS macromer. The stretching vibrations of the N—H groups at 3300 cm^{-1} together with the carbonyl bands at 1726 cm^{-1} were indicative of the presence of urethane moieties.

TABLE I
Solubility Behavior of Amine–Ester-Functionalized Macromers

Solvent	PHMS–**3a**	PHMS–**3b**	POSS–**3a**	POSS–**3b**
NMP	+	+	+	+
DMF	+	+	+	+
DMSO	+	+	+	+
DCM	−	−	−	+
THF	±	±	±	+
Toluene	−	−	−	−
Chloroform	−	−	−	+
Methanol	−	−	±	+

The quantitative solubility was tested with a 15-mg sample in 1 mL of the solvent. + = soluble at room temperature; ± = partially soluble at room temperature; − = insoluble even on heating; DCM = dichloromethane; DMF = *N*,*N*′-dimethylformamide; DMSO = dimethyl sulfoxide; NMP = *N*-methylpyrrolidone; THF = tetrahydrofuran.

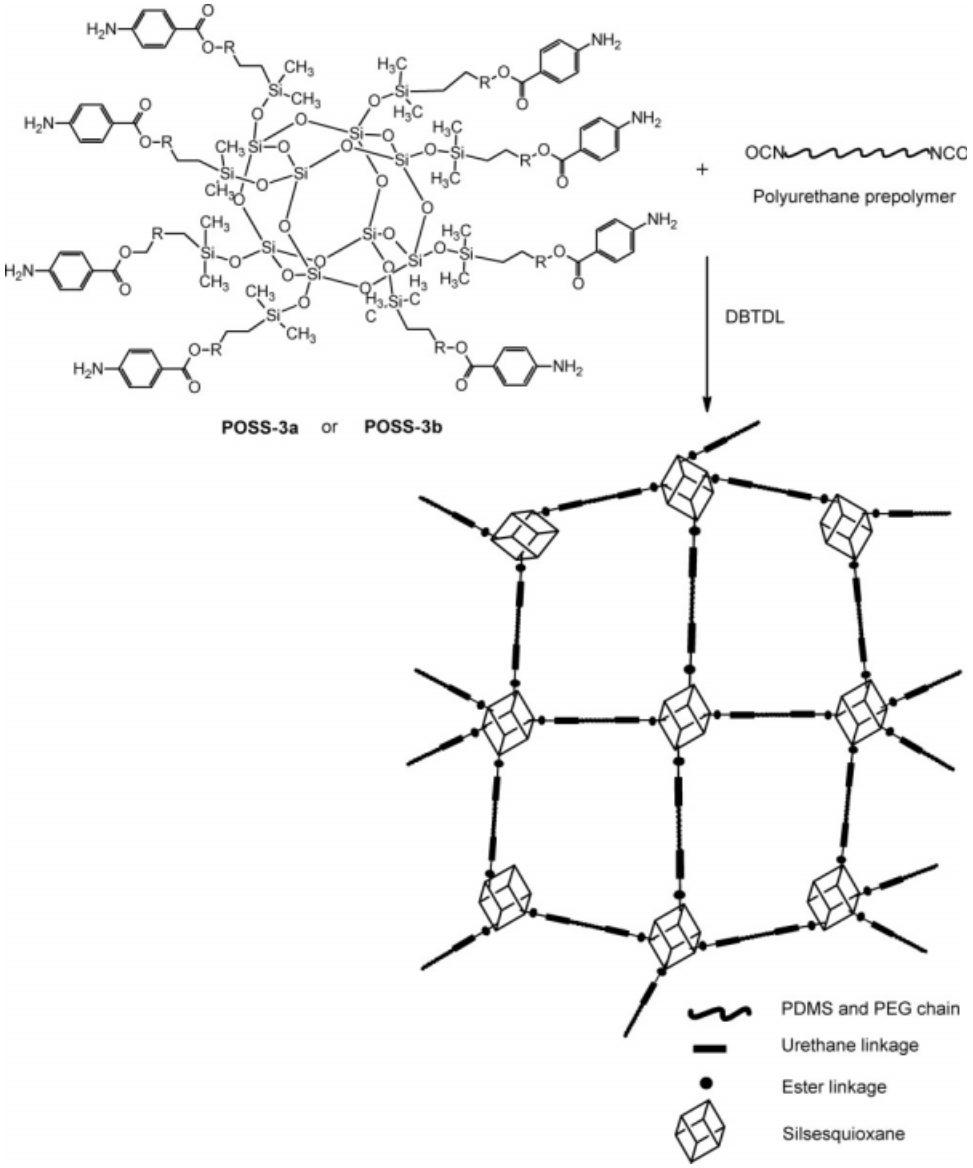

Scheme 4 Synthesis of PU–POSS–**3a** and PU–POSS–**3b**.

Multiple absorption spectra were observed near 1750–1630 cm^{-1}, and they reflected the properties of hydrogen bonding in the hybrid films. All the spectra were characterized by a major band centered at approximately 1725 cm^{-1}, which was attributed to free C=O urethane groups, and a shoulder at 1710 cm^{-1}, which might have been due to C=O ester groups of the macromers. A strong peak near 1635 and 1665 cm^{-1} corresponded to the free C=O urea and hydrogen-bonded urea C=O group. The band at 1116 cm^{-1} was due to the stretching vibration of Si—O—Si groups of PHMS and POSS, and the band at 1024 cm^{-1} was due to the stretching vibration of C—O—C groups of PEG. The IR analysis confirmed the disappearance of the bands at 2250–2275 cm^{-1}, which are the distinct characteristic peaks of isocyanate groups, indicating the completion of the cross-linking reaction between the macromers and the PU prepolymer.

AFM

To understand the influence of POSS nanoparticles on the final composite structure, the top surfaces of the prepared composites were observed with AFM. The surface topography of AFM images of hybrids with 10 wt % POSS ratios is shown in Figure 4(a,b). Microphase separation with granular-type POSS aggregation was observed on the surfaces of the hybrids. The heterogeneous morphology of the hybrids revealed the incompatibility of the hydrophobic POSS molecule with the PU matrix. Because

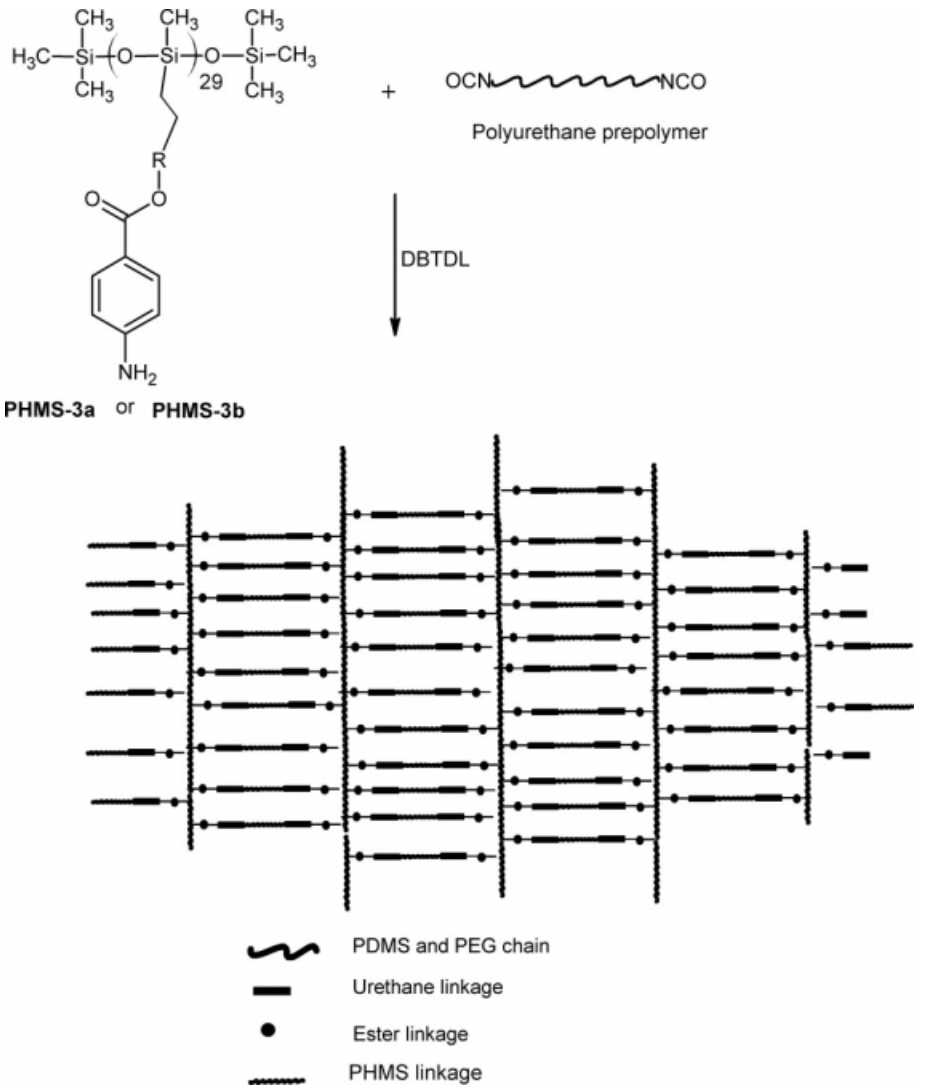

Scheme 5 Synthesis of PU–PHMS–**3a** and PU–PHMS–**3b**.

of the thermodynamic incompatibility of the POSS and PU components in the matrix, the POSS molecule aggregated on the surfaces of the hybrid membranes. The microphase-separated morphology led to very attractive bulk mechanical properties for the POSS-incorporated hybrids; this was observed by DMA, which showed enhanced mechanical properties for the POSS-incorporated hybrids. However, multiple T_g values for the microphase-separated polymer chains were not observed clearly in the DSC analysis. In practice, the amount of phase-separated material was small versus the mass of the bulk phases, so the T_g values of the microphases could not be observed readily.

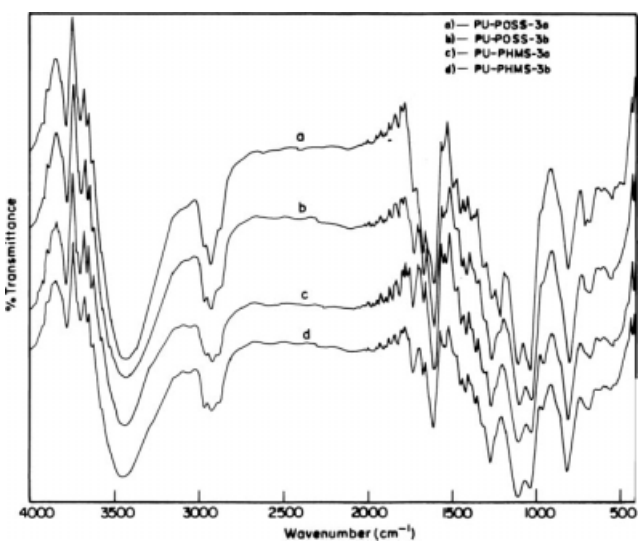

Figure 3 FTIR spectra of various macromer-incorporated PU hybrid films.

TGA

The TGA and differential thermogravimetry (DTG) curves of the obtained macromers and PU hybrid

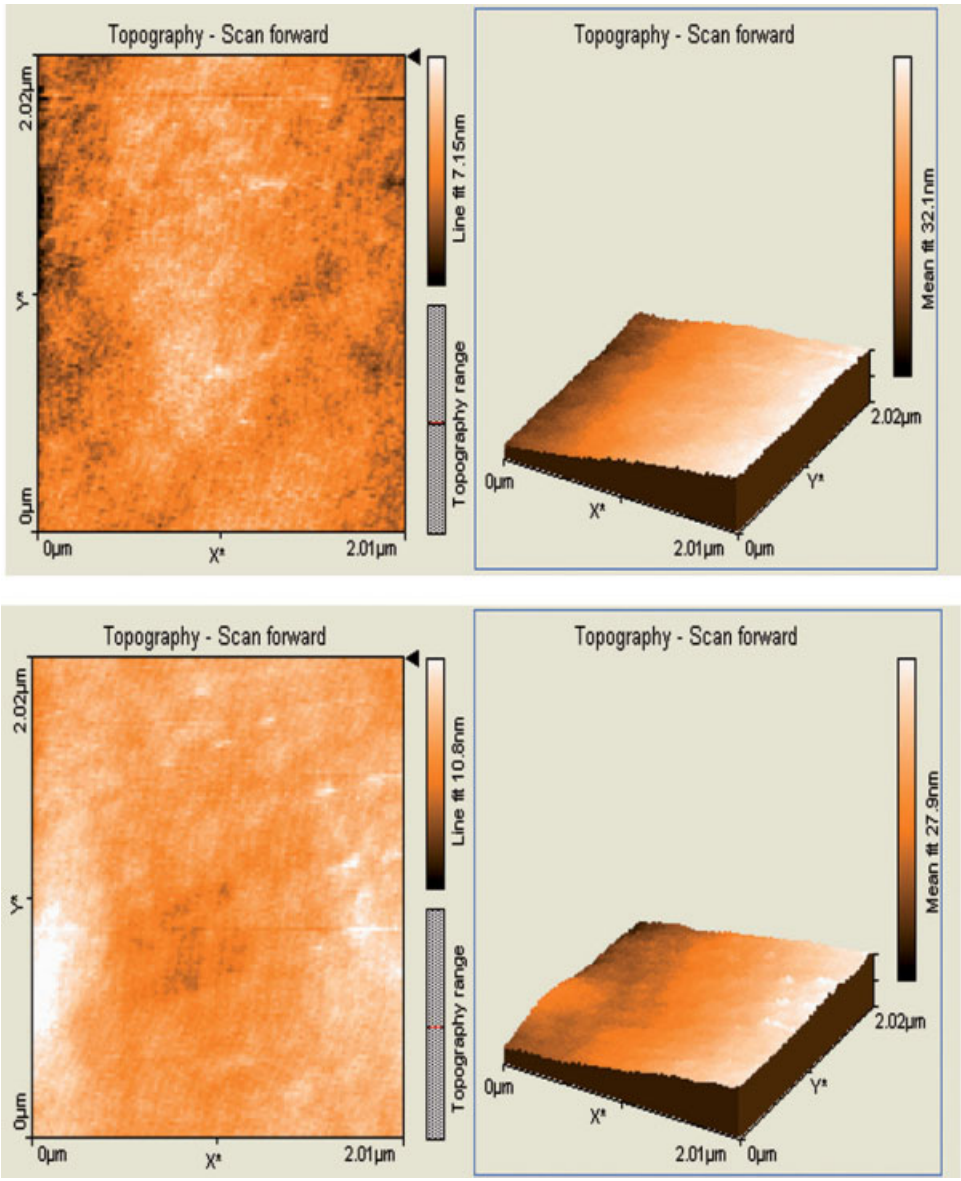

Figure 4 AFM images of PU nanohybrids: (a) PU–POSS–**3a** (top) and (b) PU–POSS–**3b** (bottom). [Color figure can be viewed in the online issue, which is available at www.interscience.wiley.com.]

films are shown in Figures 5–8. Macromers such as POSS–**3a** and PHMS–**3a** showed a two-stage decomposition process, and macromers such as POSS–**3b** and PHMS–**3b** showed single-stage decomposition thermograms. The initial decomposition of POSS–**3a** and PHMS–**3a** could have been due to the decomposition of thermally less stable organic substituents (**3a**) in the inorganic core. The second stage of decomposition was due to the decomposition of highly stable siloxane or POSS groups. TGA suggested that the macromers containing silsesquioxane were more stable than those macromers containing linear PDMS chains. The thermal stability of macromers such as POSS–**3a** and PHMS–**3a** was higher than that of POSS–**3b** and PHMS–**3b**. Also, the decomposition patterns of POSS–**3a** and PHMS–**3a** were different from those of POSS–**3b** and PHMS–**3b**. This observation implies that the thermal properties depended not only on the POSS cage or PDMS inorganic core but also on the organic tethers involved in the inorganic core.

All the PU hybrids showed similar initial decomposition patterns, and neither PDMS nor POSS had an effect near the initial decomposition temperature. However, at a higher temperature range, the decomposition patterns of POSS-incorporated PU hybrids differed slightly from those of PDMS-incorporated PU hybrids, and the char yield values were also high for POSS-incorporated PU hybrids. However, at a higher temperature range, the decomposition

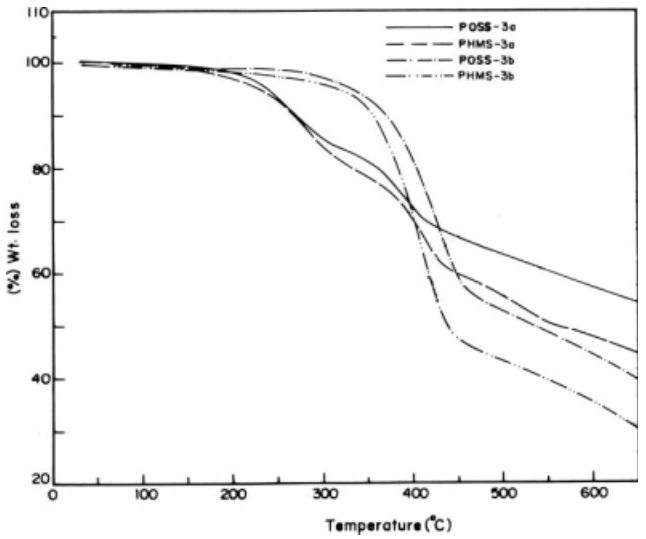

Figure 5 TGA curves of macromers at a heating rate of 5°C/min under nitrogen.

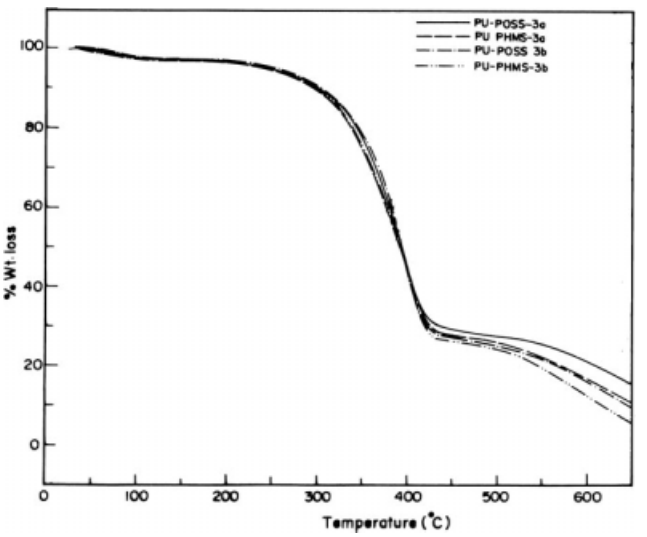

Figure 7 TGA curves of PU hybrid films at a heating rate of 5°C/min under nitrogen.

patterns of POSS-incorporated PU hybrids differed slightly from those of PDMS-incorporated PU hybrids, and the char yield values were also high for POSS-incorporated PU hybrids. The average E_a values of PU hybrids, calculated with the Ozawa method[38] at various heating rates, are shown in Table II. E_a depended on the kinds of crosslinkers used for the synthesis of the hybrids. The E_a values of the hybrids were found to be 84.22, 77.44, 75.33, and 70.33 kJ/mol for PU–POSS–**3a**, PU–POSS–**3b**, PU–PHMS–**3a**, and PU–PHMS–**3b**, respectively. Figure 9 shows a plot of the logarithm of the heating rate against the reciprocal of the absolute temperature at various degrees of conversion (α) for the PU–POSS–**3a** hybrid. The POSS-incorporated hybrids displayed E_a values higher than those of the PHMS-incorporated hybrids. At values of α (weight loss at a given temperature/total weight loss of the degradation) near the initial degradation stage ($\alpha < 0.3$), similar E_a values were observed for both types of hybrids, and this indicated that the initial degradation was due to the less thermally stable urethane/urea groups present in both types of hybrids. However, at higher α values (>0.7), high E_a values were observed for the POSS-incorporated hybrids. This revealed that at higher α values, the degradation was mainly due to the POSS or PHMS molecule, and the higher E_a values at higher α values (>0.7) for the POSS nanohybrids reflected the fact that the POSS molecule was more thermally stable than the PHMS crosslinker. On the basis of the E_a and char yield values, we could suggest that the POSS-incorporated nanohybrids possessed better thermal properties than the PDMS-incorporated PU hybrids. The decomposition values of the macromers and hybrids are presented in Table III.

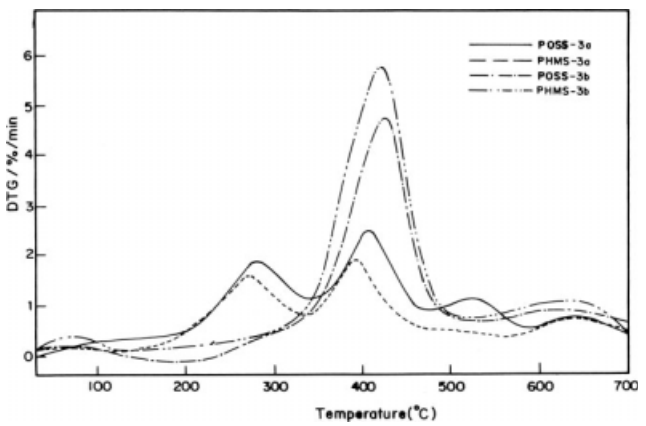

Figure 6 DTG curves of macromers at a heating rate of 5°C/min under nitrogen.

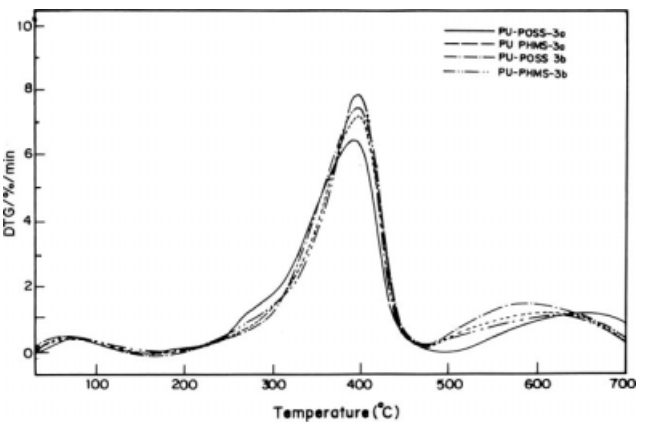

Figure 8 DTG curves of PU hybrid films at a heating rate of 5°C/min under nitrogen.

TABLE II
E_a Values for the Sample Degradation Process Calculated with the Ozawa Method

Sample	α									Average E_a (kJ/mol)
	0.1	0.2	0.3	0.4	0.5	0.6	0.7	0.8	0.9	
PU–POSS–**3a**	55	66	71	76	86	84	83	112	125	84
PU–POSS–**3b**	54	64	68	70	76	79	81	99	106	77
PU–PHMS–**3a**	54	63	65	70	75	80	77	92	102	75
PU–PHMS–**3b**	52	58	60	68	73	72	70	85	95	70

DSC analysis

The DSC curves of the macromers are shown in Figure 10. For the PDMS-functionalized macromer, T_g values were shifted from −135 (unfunctionalized PDMS) to −4 (PHMS–**3a**) and −93°C (PHMS–**3b**). The melting temperatures for PHMS–**3a** and PHMS–**3b** were observed at 159 and 5.1°C, respectively. The POSS-functionalized macromer showed an endothermic peak near 6°C for POSS–**3a** and one at −101°C for the POSS–**3b** macromer, and these might represent the T_g values. Also, these monomers showed melting temperatures of 161 and −1°C. The DSC curves of macromers such as POSS–**3a** and PHMS–**3a** showed similar thermogram patterns, and similar observations were made for the POSS–**3b** and PHMS–**3b** macromers. These observations indicated that the transitions in the macromer mainly depended on the functional group substituted into the siloxane groups.

Figure 11 shows the DSC thermograms of the PU hybrids obtained with POSS nanoparticles and PDMS-functionalized macromers. All the hybrids showed a single T_g value, and this suggested that these hybrids exhibited a single phase. The T_g values of the nanohybrids were significantly increased in comparison with those of the hybrids obtained with the linear PDMS macromer. The enhanced T_g values resulted from the restricted motion of the polymer chains, which was caused by the even distribution of POSS units on the segmental level. The nanohybrids showed T_g values of 45 and 39°C for PU–POSS–**3a** and PU–POSS–**3b**, respectively. The PDMS-macromer-incorporated PU hybrids showed T_g values of 27 and 25°C. The T_g values of PU hybrids obtained with the PDMS chain macromer were expected to be high because the number of crosslinking sites was high in the PDMS macromer. However, this trend was not observed, and the T_g values of the nanohybrids were higher than those of the PDMS-incorporated hybrids. This indicated that the restriction of the segmental mobility by the hard cage structure of POSS was more predominant than the crosslinking density of the PU hybrids. Therefore, one may presume that the structural arrangement of the silicon atom played a more important role than the crosslinking density in the hybrids.

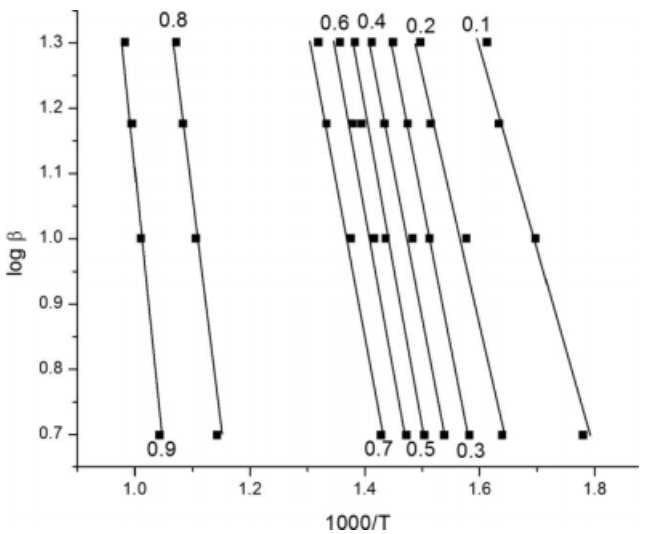

Figure 9 Plot of the logarithm of the heating rate (log β) against the reciprocal of the absolute temperature (1000/T) at various α values for the PU–POSS–**3a** hybrid.

DMA

A plot of the storage modulus (E') as a function of temperature at 0.1 Hz for the PU hybrids is shown in Figure 12. E' was increased by the incorporation of a small amount of POSS into the hybrid. The E' values of all the POSS hybrids were higher than those of the linear-PDMS-chain-incorporated hybrids. The E' values at 30°C were found to be 190.17, 118.76,

TABLE III
TGA and DSC Values for the Macromers and PU Hybrids

Sample	T_{10} (°C)	T_{50} (°C)	Char yield at 650°C (%)	T_g (°C)
POSS–**3a**	239	684	53.8	6
POSS–**3b**	339	500	39.4	−101
PHMS–**3a**	236	524	44.2	4
PHMS–**3b**	323	407	30.0	−93
PU–POSS–**3a**	294	393	15.2	45
PU–POSS–**3b**	301	395	13.2	39
PU–PHMS–**3a**	300	395	7.48	27
PU–PHMS–**3b**	300	392	5.5	25

T_{10} = temperature at 10% decomposition; T_{50} = temperature at 50% decomposition.

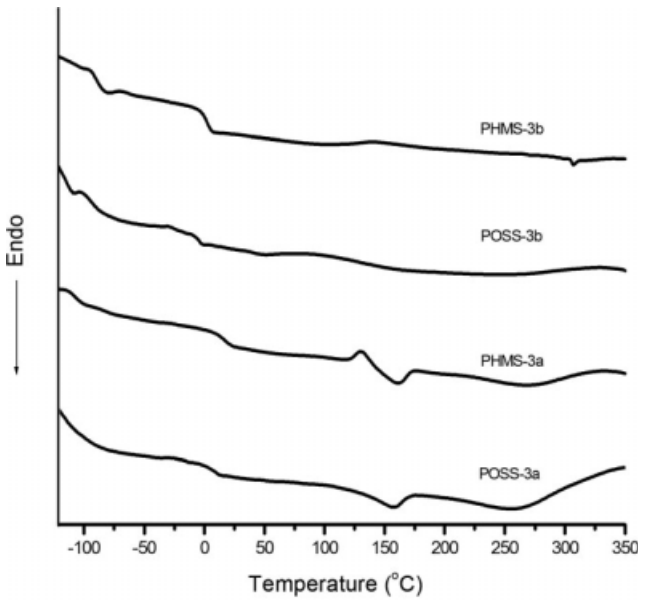

Figure 10 DSC curves of macromers.

40.43, and 22.25 MPa for PU–POSS–**3a**, PU–POSS–**3b**, PU–PHMS–**3a**, and PU–PHMS–**3b**, respectively. The POSS-incorporated hybrids had E' values 4 times greater than those of the linear-PDMS-chain-incorporated hybrids. This implied that the incorporation of the POSS nanoparticle played an important role in the viscoelastic behavior of the synthesized hybrids. The hybrids showed a very long range rubbery plateau region because all the hybrids contained almost 90% concentrations of both the PEG and PDMS soft segments. The enormous increase in E' of the nanohybrids even at a low concentration (10 wt %) of POSS incorporation confirmed the contribution of the POSS cage structure toward the increase in the viscoelastic properties of the nanohybrids. Figure 13 shows plots of tan δ as a function of temperature for the PU hybrids obtained from the POSS macromer and linear PHMS macromer. T_g (tan δ peak temperatures) was observed at 44, 37, 29, and 20°C for PU–POSS–**3a**, PU–POSS–**3b**, PU–PHMS–**3a**, and PU–PHMS–**3b**, respectively. The T_g values significantly increased with an increase in the incorporation of POSS, as explained by the DSC analysis. The T_g values obtained from DSC measurements were found to be in good agreement with the T_g values obtained from DMA measurements. For the POSS-incorporated PU hybrids, the tan δ values were very high and the peaks were broadened in comparison with the PDMS-incorporated PU hybrids. The high δ peaks showed an even distribution of POSS molecules in the PU network structure.

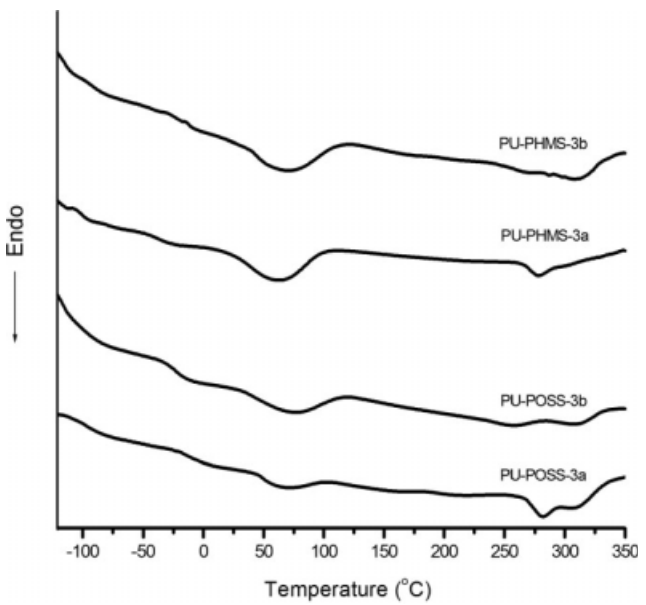

Figure 11 DSC curves of PU hybrid films.

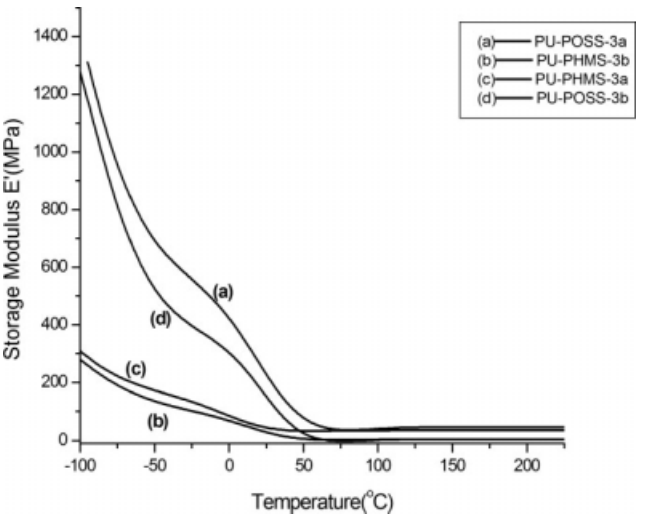

Figure 12 Plot of E' versus the temperature for PU hybrid films.

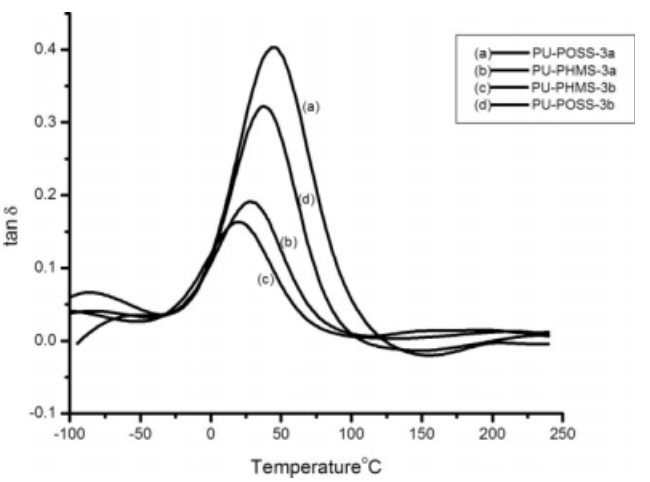

Figure 13 Plot of tan δ versus the temperature for PU hybrid films.

CONCLUSIONS

A new class of ester–amine-functionalized silsesquioxane macromers was synthesized, and these macromers were used to synthesize PU nanocomposites. Similarly, an ester–amine-functionalized linear poly(dimethylsiloxane) was also synthesized to study the influence of the silsesquioxane macromer and PDMS macromer on the thermal and mechanical properties of PU hybrids. AFM images showed a heterogeneous morphology reflecting the less dispersive nature of POSS with the PU hybrids. The TGA thermograms of the macromers revealed that the thermal stability depended on both the substituted functional group and the structure of the siloxane compound. The DSC curves of the macromers showed that the thermal transitions were mainly dependent on the functional group substituted into the inorganic core. The T_g values of the POSS-incorporated PU networks were higher than those of the linear-PDMS-chain-incorporated PU networks, and this showed that the restriction of segmental mobility was highly influenced by the POSS cage structure. The mechanical properties of the POSS-incorporated network showed an enhancement of E'.

References

1. Queiroz, D. P.; De-Pinho, M. N. Polymer 2005, 46, 2346.
2. Stanciu, A.; Airinei, A.; Oprea, S. Polymer 2001, 42, 6081.
3. Sonnenschein, M. F.; Lysenko, Z.; Brune, D. A.; Wendt, B. L.; Schrock, A. K. Polymer 2005, 46, 10158.
4. Wang, L. F.; Ji, Q.; Glass, T. E.; Ward, T. C.; McGrath, J. E.; Muggli, M.; Burns, G.; Sorathia, U. Polymer 2000, 41, 5083.
5. Yeganeh, H.; Shamekhi, M. A. Polymer 2004, 45, 359.
6. Lee, A.; Lichtenhan, J. D. J Appl Polym Sci 1999, 73, 1993.
7. Zheng, J.; Ozisik, R.; Siegel, R. W. Polymer 2005, 46, 10873.
8. Pattanayak, A.; Jana, S. C. Polymer 2005, 46, 3275.
9. Neumann, D.; Fisher, M.; Tran, L.; Matisons, J. G. J Am Chem Soc 2002, 124, 13998.
10. Liu, H.; Zheng, S. Macromol Rapid Commun 2005, 26, 196.
11. Mya, K. Y.; He, C.; Huang, J.; Xiao, Y.; Dai, J.; Siow, Y. P. J Polym Sci Part A: Polym Chem 2004, 42, 3490.
12. Lee, L. H.; Chen, W.-C. Polymer 2005, 46, 2163.
13. Baney, R. H.; Itoh, M.; Sakakibara, A.; Suzuki, T. Chem Rev 1995, 95, 1409.
14. Zhang, Y.; Lee, S.; Yoonessi, M.; Liang, K.; Pittman, C. U. Polymer 2006, 47, 2984.
15. Choi, J.; Yee, A. F.; Laine, R. M. Macromolecules 2003, 36, 5666.
16. Cardoen, G.; Coughlin, E. B. Macromolecules 2004, 37, 5123.
17. Yoon, K. W.; Polk, M. B.; Park, J. H.; Min, B. G.; Schiraldi, D. A. Polym Int 2005, 54, 47.
18. Liang, K.; Li, G.; Toghiani, H.; Koo, J. H.; Pittman, C. U., Jr. Chem Mater 2006, 18, 301.
19. Feher, F. J. Chem Commun 1998, 399.
20. Schwab, J. J.; Lichtenhan, J. D. Appl Organomet Chem 1998, 12, 707.
21. Huang, J. C.; He, C. B.; Xiao, Y.; Mya, K. Y.; Dai, J.; Siow, Y. P. Polymer 2003, 44, 4491.
22. Costa, R. O. R.; Vasconcelos, W. L.; Tamaki, R.; Laine, R. M. Macromolecules 2001, 34, 5398.
23. Lee, Y. J.; Huang, J. M.; Kuo, S. W.; Lu, J. S.; Chang, F. C. Polymer 2005, 46, 173.
24. Feher, F. J.; Blanski, R. L. J Chem Soc Chem Commun 1990, 1614.
25. Kannan, R. Y.; Salacinski, H. J.; Groot, J. D.; Clatworthy, I.; Bozec, L.; Horton, M.; Butler, P. E.; Seifalian, A. M. Biomacromolecules 2006, 7, 215.
26. Choi, J.; Harcup, J.; Yee, A. F.; Zhu, Q.; Laine, R. M. J Am Chem Soc 2001, 123, 11420.
27. Tamaki, R.; Tanaka, Y.; Asuncion, M. Z.; Choi, J.; Laine, R. M. J Am Chem Soc 2001, 123, 12416.
28. Zhang, C.; Laine., R. M. J Am Chem Soc 2000, 122, 6979.
29. Zhang, C.; Babonneau, F.; Bonhomme, C.; Laine, R. M.; Soles, C. L.; Hristov, H. A.; Yee, A. F. J Am Chem Soc 1998, 120, 8380.
30. Lin, H. C.; Kuo, S. W.; Huang, C. F.; Chang, F. C. Macromol Rapid Commun 2006, 27, 537.
31. Liu, Y.; Ni, Y.; Zheng, S. Macromol Chem Phys 2006, 207, 1842.
32. Fu, B. X.; Hsiao, B. S.; Pagola, S.; Stephens, P.; White, H.; Rafailovich, M.; Sokolov, J.; Mather, P. T.; Jeon, H. G.; Phillips, S.; Lichtenhan, J.; Schwab, J. Polymer 2001, 42, 599.
33. Fu, B. X.; Hsiao, B. S.; White, H.; Rafailovich, M.; Mather, P. T.; Jeon, H. G.; Phillips, S.; Lichtenhan, J.; Schwab, J. Polym Int 2000, 49, 437.
34. Oaten, M.; Choudhury, N. M. Macromolecules 2005, 38, 6392.
35. Hasegawa, I. J Sol-Gel Sci Technol 1993, 1, 57.
36. Hasegawa, I.; Motojima, D. J Organomet Chem 1992, 44, 373.
37. Park, H. B.; Kim, C. K.; Lee, Y. M. J Membr Sci 2002, 204, 257.
38. Ozawa, T. Bull Chem Soc Jpn 1965, 38, 1881.